JOURNAL OF VIROLOGY, Aug. 1994, p. 5117–5125
0022-538X/94/$04.00+0

Vol. 68, No. 8

Three-Dimensional Structure of Baculovirus-Expressed Norwalk Virus Capsids

B. V. VENKATARAM PRASAD,[1]* R. ROTHNAGEL,[1] XI JIANG,[2]† AND M. K. ESTES[2]

Verna and Marrs Mclean Department of Biochemistry and W. M. Keck Center for Computational Biology,[1] and Division of Molecular Virology,[2] Baylor College of Medicine, Houston, Texas 77030

Received 3 January 1994/Accepted 25 April 1994

The three-dimensional structure of the baculovirus-expressed Norwalk virus capsid has been determined to a resolution of 2.2 nm using electron cryomicroscopy and computer image processing techniques. The empty capsid, 38.0 nm in diameter, exhibits T=3 icosahedral symmetry and is composed of 90 dimers of the capsid protein. The striking features of the capsid structure are arch-like capsomeres, at the local and strict 2-fold axes, formed by dimers of the capsid protein and large hollows at the icosahedral 5- and 3-fold axes. Despite its distinctive architecture, the Norwalk virus capsid has several similarities with the structures of T=3 single-stranded RNA (ssRNA) viruses. The structure of the protein subunit appears to be modular with three distinct domains: the distal globular domain (P2) that appears bilobed, a central stem domain (P1), and a lower shell domain (S). The distal domains of the 2-fold related subunits interact with each other to form the top of the arch. The lower domains of the adjacent subunits associate tightly to form a continuous shell between the radii of 11.0 and 15.0 nm. No significant mass density is observed below the radius of 11.0 nm. It is suspected that the hinge peptide in the adjoining region between the central domain and the shell domain may facilitate the subunits adapting to various quasiequivalent environments. Architectural similarities between the Norwalk virus capsid and the other ssRNA viruses have suggested a possible domain organization along the primary sequence of the Norwalk virus capsid protein. It is suggested that the N-terminal 250 residues constitute the lower shell domain (S) with an eight-strand β-barrel structure and that the C-terminal residues beyond 250 constitute the protruding (P1+P2) domains. A lack of an N-terminal basic region and the ability of the Norwalk virus capsid protein to form empty T=3 shells suggest that the assembly pathway and the RNA packing mechanisms may be different from those proposed for tomato bushy stunt virus and southern bean mosaic virus but similar to that in tymoviruses and comoviruses.

Norwalk virus is a member of the *Caliciviridae* and an important human pathogen that causes epidemic acute gastroenteritis in humans (27, 30). It has been estimated that about 42% of outbreaks of acute, epidemic nonbacterial gastroenteritis in the United States are caused by Norwalk virus and Norwalk-like viruses including Hawaii, Snow Mountain, and Montgomery County viruses (6, 31). Although the Norwalk virus was identified 20 years ago, progress in understanding the molecular characteristics of the virus and its replication strategies have been hampered by the lack of a cell culture system or a practical animal model. The only source of the virus has been stool samples from volunteers infected with Norwalk virus. The yield of virus from such stool samples is extremely low, and virus is rarely seen in stools unless immune electron microscopy is performed (30). Recent success in cloning the Norwalk virus genome and its expression in the baculovirus system is paving the way for a better understanding of the epidemiological, immunological, biochemical, and other functional properties of the virus (17, 18, 26–29, 32, 34, 35, 50).

Norwalk virus contains a genome of positive-sense single-stranded RNA (ssRNA) of about 7.7 kb (29). Three open reading frames (ORFs) in the genome have been identified (29). The first ORF codes for a polyprotein and contains regions of amino acid similarity to the 2C helicase, 3C protease of poliovirus, and a 3D RNA-dependent RNA polymerase similar to other ssRNA viruses; the second ORF encodes the capsid protein (apparent molecular weight, 58,000 [28]); and the third ORF codes for a protein whose functional properties are not yet clear. The presence of multiple ORFs and the single capsid protein are distinctive features of the members of the *Caliciviridae* which include the prototype vesicular exanthema virus, feline calicivirus, San Miguel sea lion virus, the primate calicivirus, and the rabbit hemorrhagic virus (reviewed in reference 7). These features contrast with those of the picornaviruses which code for a single ORF encoding a polyprotein that undergoes posttranslational cleavages to produce smaller structural (VP1, VP2, VP3, and VP4) and nonstructural proteins. All the caliciviruses possess a single capsid protein with apparent molecular weights ranging from 59,000 to 65,000. While common among plant viruses, virus capsids made of a single-structure protein are unusual among animal viruses. The only other known example until now, apart from caliciviruses, is nodaviruses (22, 25).

We have undertaken three-dimensional structural studies of the members of the *Caliciviridae* to establish structure-function relationships and to understand their architectural principles, particularly in comparison with the known structures of other ssRNA viruses. We have carried out three-dimensional structural studies of baculovirus-expressed Norwalk virus capsids, in lieu of native Norwalk virus, which currently cannot be obtained in large quantities. When expressed with the baculovirus system, the capsid protein of the Norwalk virus spontaneously assembles into virus-like particles (28). These particles are expressed and can be purified in large quantities. We present here the three-dimensional structure of the baculovirus-expressed Norwalk virus capsid determined by electron cryomi-

* Corresponding author. Phone: (713) 798-5686. Fax: (713) 796-9438. Electronic mail address: vprasad@bcm.tmc.edu.

† Present address: Center for Pediatric Research, Eastern Virginia Medical School, Norfolk, VA 23510-1001.

croscopy and computer image processing techniques to a nominal resolution of 2.2 nm.

MATERIALS AND METHODS

Purification of rNV capsids from infected insect cells. The recombinant Norwalk virus (rNV) particles were produced and purified from insect cells infected with a recombinant baculovirus that contains the 3′ end of the viral genome as previously described (28). Supernatants of rNV baculovirus-infected cell cultures were extracted once with trichlorofluroethane (genetron). The virus capsids then were pelleted by centrifugation at 27,000 rpm for 90 min in an SW 28 rotor (Beckman). The resultant pellets were suspended in water and loaded onto a discontinuous sucrose gradient (10 to 50%) and centrifuged at 25,000 rpm for 1 h in an SW 28 rotor. The gradients were fractionated by bottom puncture, and 0.5 ml of each fraction was collected. Aliquots of each fraction were assayed for the viral capsid protein by polyacrylamide gel electrophoresis and then by staining the gel with Coomassie blue. The peak fractions containing the 58-kDa viral capsid protein were pooled, and the sucrose was removed by dilution of the sample with water followed by centrifugation at 27,000 rpm for 90 min in an SW 28 rotor. The resultant pellets were suspended in a solution of CsCl (1.362 g/ml) and centrifuged to equilibrium at 35,000 rpm for 24 h in a Beckman SW 50.1 rotor. The viral capsids containing the 58-kDa capsid protein were identified by electrophoretic analysis of aliquots of the fractions from the gradient. The peak fractions of the viral capsids were pooled and pelleted by centrifugation for 2 h at 35,000 rpm in a Beckman SW 50.1 rotor to remove the CsCl. For high purity of the viral capsids, a second CsCl gradient purification was carried out. The peak fractions of the second CsCl gradient were pooled, pelleted, and suspended in water for electron cryomicroscopy.

Electron cryomicroscopy. The rNV particles were embedded in a thin layer of vitreous ice over holes on a holey carbon grid by established procedures (3, 13, 42–44). The specimen grid was transferred via a Gatan workstation into a JEOL 1200 microscope and examined at −155°C. Images were recorded with electron doses of 400 to 600 electrons per nm^2 per image at a magnification of ×30,000. A set of two micrographs was recorded from each specimen area: the first was underfocused by 1 μm and the next by 2 μm. The 2-μm images were used to confirm the orientations of the particles, and the 1-μm images were used in the three-dimensional reconstructions.

Computer image processing. The three-dimensional structure was reconstructed from the electron cryomicrographs by procedures described previously (5, 10, 16, 42–44). The electron micrographs were digitized on a scanning densitometer with a step size corresponding to 0.533 nm in the object. The orientations of the rNV capsids were determined by the common lines procedure (10, 16). Once the orientations of the particles were determined, the phase origins of the particles were refined. Refinement of the origin and particle orientation was carried out iteratively until no changes occurred in either of them. The orientation parameters and the phase origin of each particle then were further refined with respect to the entire data set, using cross-common lines (16, 42). When particles adequate to sample the asymmetric unit of the icosahedron were available, an initial three-dimensional reconstruction was computed by cylindrical expansion methods, imposing a lower 522 symmetry (10, 11). This three-dimensional density map was projected along the orientation parameters of the particles, and the respective projected maps were cross-correlated with the images to determine the phase centers more precisely. After another cycle of refinement of the orientations of the particles by using cross-common lines with these phase centers, the final three-dimensional map was reconstructed to a nominal resolution of 2.2 nm. No corrections due to contrast transfer function were incorporated in the reconstruction. The radial density plots were computed from the three-dimensional density maps by averaging the densities in concentric shells of 0.533 nm width about the center of the map. All the computations were carried out on Silicon Graphics workstations. The visualization of the three-dimensional density maps and the computer graphics was carried out with the EXPLORER software from Silicon Graphics, Inc.

RESULTS

Electron cryomicroscopy and image analysis. Electron cryomicrographs of the rNV particles embedded in ice and recorded at 1 and 2 μm underfocus are shown in Fig. 1. The particles are empty spherical shells, measuring 38.0 nm in diameter, with a rough outer surface. In the higher defocus image (Fig. 1b), the low-resolution features are accentuated. The protein density is seen between the radius of 11.0 and 19.0 nm. Small projections emanating from a smooth rim of about 4.0 nm in thickness are apparent in most of the particles.

The three-dimensional structure of rNV capsid was determined by using 27 particles in unique orientations. These particles were chosen from the micrograph recorded with an underfocus value of 1 μm. The orientation parameters of these particles are shown in Fig. 2. The extent to which the data from these particles obey the expected icosahedral symmetry is evaluated by computing the mean phase difference (phase residual) for all pairwise particle comparisons at regular intervals along the cross-common lines in the Fourier transforms of the respective particles (10, 16). Phase residual greater than 90°, a value for randomized phases, indicates no correlation with icosahedral symmetry. The phase residual plot as a function of resolution for our data is shown Fig. 3. The overall phase residual for the entire data out to 2.2-nm resolution is around 45°. The phase residual is significantly less than 90° for most of the data and approaches 90° for data around ~2.2-nm resolution. The resolution limit, ~2.2 nm, of the icosahedral correlation is consistent with the defocus level (1 μm) of the micrograph.

T=3 icosahedral symmetry. The three-dimensional structure of the Norwalk virus capsid exhibits icosahedral symmetry. Surface representations of the three-dimensional structure along the icosahedral 5- and 3-fold axes are shown in Fig. 4. Although a lower 522 symmetry was used in the reconstruction procedure, the reconstruction showed excellent 532 symmetry. As a further check on the reliability of the reconstruction, the input images were compared with the projections obtained from the three-dimensional density map in orientations corresponding to the images. The arrangement of the mass density is prototypical of a T=3 icosahedral lattice. In such a lattice, the neighboring 5-fold axes of symmetry are related by one 6-coordinated position coincident with the icosahedral 3-fold axis (8).

Arch-like capsomeres. The main feature of the three-dimensional structure of rNV particles is the presence of 90 arch-like capsomeres located at all the local and strict 2-fold axes of the T=3 icosahedral lattice. These capsomeres are arranged in such a way that there are prominent hollows at all the icosahedral 5- and 3-fold axes (Fig. 4). The arches begin at a radius of 15.0 nm and extend to a radius of about 19.0 nm. A rectangular platform of ~5.0 by 7.0 nm is located at the top of the arch. The hole between the two sides of the arch is about

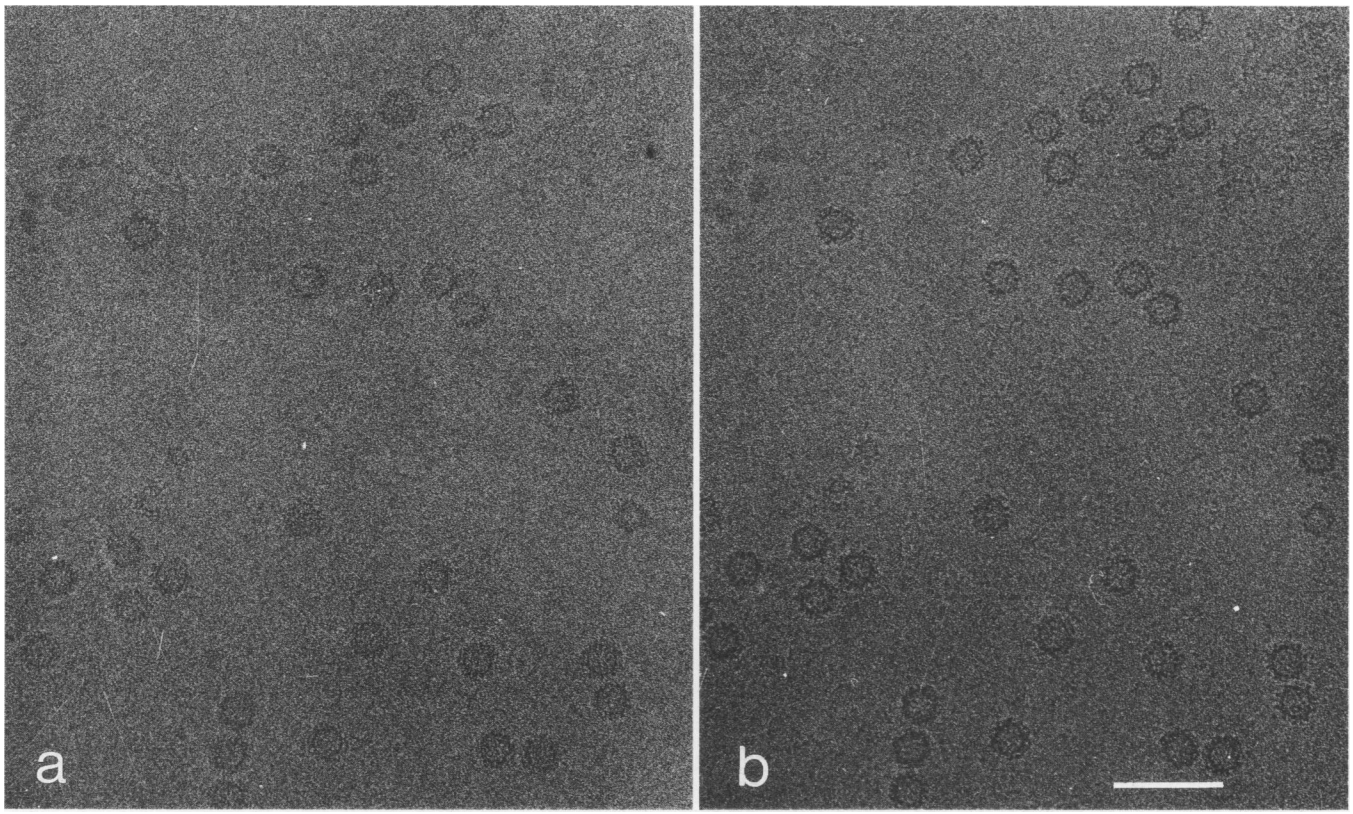

FIG. 1. Electron cryomicrographs of baculovirus-expressed Norwalk virus (rNV) capsids embedded in a thin layer of vitreous ice recorded at 1 (a) and 2 (b) μm underfocus. Bar, 100 nm.

2.0 nm in diameter. These arches surround the hollows which are about 4.0 nm deep and 9.0 nm wide. Each virus particle has 32 such hollows, 12 of which are on the icosahedral 5-fold axes, with the remaining 20 hollows at the icosahedral 3-fold axes. The hollows at the 5-fold axes have a small hump at the center with a mote around it, while the hollows at the icosahedral 3-fold positions are rather flat.

Two types of capsomeres. The 90 capsomeres can be classified into two types on the basis of their locations with respect to the icosahedral axes of symmetry (Fig. 5). The first type of capsomere, designated type A, includes the capsomeres surrounding the icosahedral 5-fold axis. These are located at the local 2-fold axes, midway between the icosahedral 5- and 3-fold positions. The second type, designated type B, includes the capsomeres located at all the strict 2-fold axes of the icosahedral structure (midway between any two neighboring 5-fold or 3-fold axes). The plane of a type A arch lies obliquely to the line joining the neighboring 5- and 3-fold axes. Similarly, the plane of a type B arch lies obliquely to the line joining the neighboring 3-fold axes. There are noticeable differences in the local environments of these capsomere types. Each type A capsomere is surrounded by two type B and two type A capsomeres (Fig. 5a), while each type B capsomere is surrounded by four type A capsomeres (Fig. 5b). There is a significant difference between the A to A and A to B distances; the A to A distance is about 8.0 nm, and the A to B distance is about 7.0 nm.

The two sides of a type B arch, each referred to as a B1 subunit, are equivalent because they are related to one another by the strict 2-fold axis. However, the two sides of the type A arch, referred to as A1 and A2 subunits, related by a local 2-fold axis, are not strictly equivalent. In the type A arch, the A1 side is closer to the 5-fold axis and the A2 side is closer to the icosahedral 3-fold axis. Each B1 side is closer to an icosahedral 3-fold axis. Despite these noticeable differences, A1, A2, and B1 subunits share common structural features including (i) a globular head region (P2), which appears bilobed, and (ii) a connecting stem region (P1), which merges into a contiguous mass density (S) at a lower radius. The head region (P2) has an overall diameter of about 3.0 nm. The connecting stem region (P1) has a diameter of about 2.5 nm. These structural features in the three subunits are shown in Fig. 6. The distal globular P2 regions of the 2-fold related subunits interact sidewards to form the rectangular platform of the arches.

Interconnections between the capsomeres. One interesting feature of the capsid structure is that the capsomeres are interlinked to one another across the lattice through a slender mass density that emanates from the two corners of the rectangular platform of the arch (Fig. 4 and 5). While the type A capsomere has two such connections at the diagonally opposite corners of the rectangular platform, the type B capsomere has such interconnections at all four corners. It can be envisaged that each subunit (A1, A2, and B1) has a sideward-protruding knob, on one side of the distal globular domain (P2), that connects with the subunit of the neighboring capsomere. We have carried out several independent reconstructions from different micrographs and at different defocus levels to confirm the presence of these interconnecting mass densities.

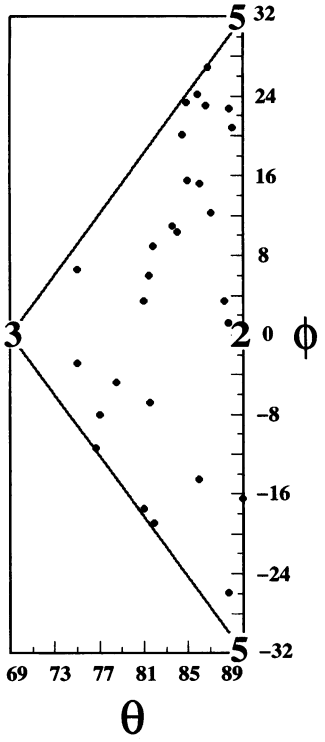

FIG. 2. Refined orientation parameters, Θ and φ, of the 24 rNV particles used in the three-dimensional structure determination. The Θ and φ are defined as in reference 33. The triangle represents the icosahedral asymmetric unit. The locations of the icosahedral (5, 3, and 2) symmetry axes in this triangle are shown.

The inner shell. The lower portions of the capsid subunits associate together to form a contiguous shell between the radii 11.5 and 15.0 nm. The bases of the hollows observed at the 5- and icosahedral 3-fold axes are parts of this shell. The base of the hollow at the 5-fold axis is formed by the close interaction between the lower portions of the A1 subunits (Fig. 7a). Similarly, the lower portions of the alternating three A2 and three B1 sides associate to form the base of the hollow at the strict 3-fold position (Fig. 7b). A surface representation of the mass density at the radius of 16.0 nm is shown in Fig. 7c. At this radius, we can still see the remnants of lower portions of the P1 domains. However, at the radius of 15.0 nm, we see a relatively smooth surface of the inner shell. The continuity of the inner shell is clearly evident in the equatorial section extracted from the entire three-dimensional density map (Fig. 7d). The arches emanate from this continuous mass density. Thus, the inner shell seems to provide a scaffolding for the arches. At the present resolution, we have not seen any holes that penetrate the inner shell. It appears that the inside of the capsid is inaccessible to the outside.

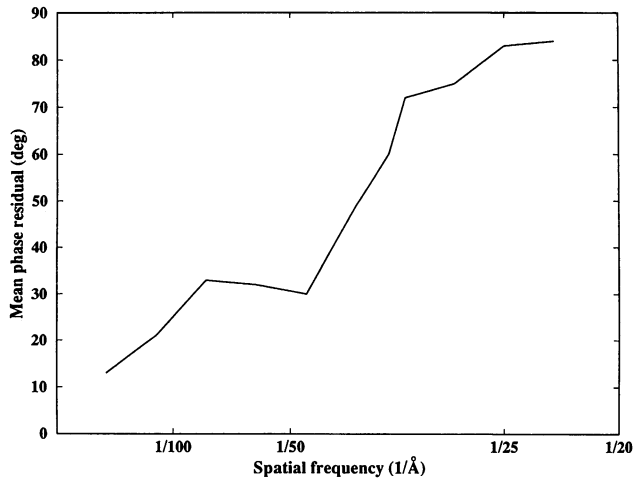

FIG. 3. Plot of the average phase residual as a function of resolution. 1 Å = 0.1 nm.

Radial density plot. The mass density distribution in the three-dimensional reconstruction of rNV capsid as a function of radius is shown in Fig. 8. This plot suggests that the mass density in the three-dimensional structure is distributed into two concentric shells: the first between the radii of 15.0 and 19.0 nm, and the second between 11.0 and 15.0 nm. The negative peak at the radius of about 19.5 nm signifies the virion boundary. This negative peak is due to the Fresnel fringes resulting from the relatively high underfocus (1 μm) employed during recording of the electron micrographs. The tops of the arches contribute to the peak at the radius of 18.5 nm; the stems of the arches, between the radii of 15.0 and 17.5 nm, contribute relatively less to the average radial density. The mass density between the radii of 11.5 and 15.0 nm is due to the inner shell described in the previous paragraph. The radial density plot clearly indicates that there is no significant mass density below the radius of 11.0 nm.

DISCUSSION

T=3 icosahedral structure. Norwalk virus, like many other ssRNA viruses, exhibits T=3 icosahedral symmetry. The three-dimensional structures of several ssRNA viruses have been determined to atomic resolution. The list includes viruses of plant origin, such as tomato bushy stunt virus (TBSV) (21), southern bean mosaic virus (SBMV) (1), turnip crinkle virus (TCV) (24), and cowpea mosaic virus (9); viruses of animal origin, such as rhinovirus (45), poliovirus (23), mengovirus (37), and foot-and-mouth disease virus (2); and insect viruses, such as black beetle virus (25) and Flock House virus (15). All these viruses, except picornaviruses and comoviruses, exhibit T=3 symmetry. The picornaviruses exhibit T=1 icosahedral symmetry. If we ignore the distinction between VP1, VP2, and VP3, which make the capsid structure with 60 copies each, we could describe the structure of picornaviruses as having a pseudo T=3 structure. The comovirus capsid, formed by two proteins, has a pseudo T=3 structure (9).

In its architecture, rNV particles show more similarities with TBSV and TCV than with other T=3 viruses. Unlike other known T=3 virus structures, the TBSV and TCV capsid proteins form prominent projections in their structures, as seen in the rNV structure. These projections form the main feature in their electron micrographs. In the other T=3 structures, however, these projections are not as obvious. One common feature of the ssRNA viruses which show true T=3 symmetry is that their capsids are made of a single structural protein, as is Norwalk virus. However, the molecular weight of the capsid protein in the rNV structure is significantly larger than those in the other T=3 structures. Consequently, the rNV structure, 38.0 nm in diameter, is significantly larger than the other T=3 structures; TBSV and TCV are about 32.5 to 35.0 nm in diameter, whereas the other T=3 structures are around 30.0 nm in diameter.

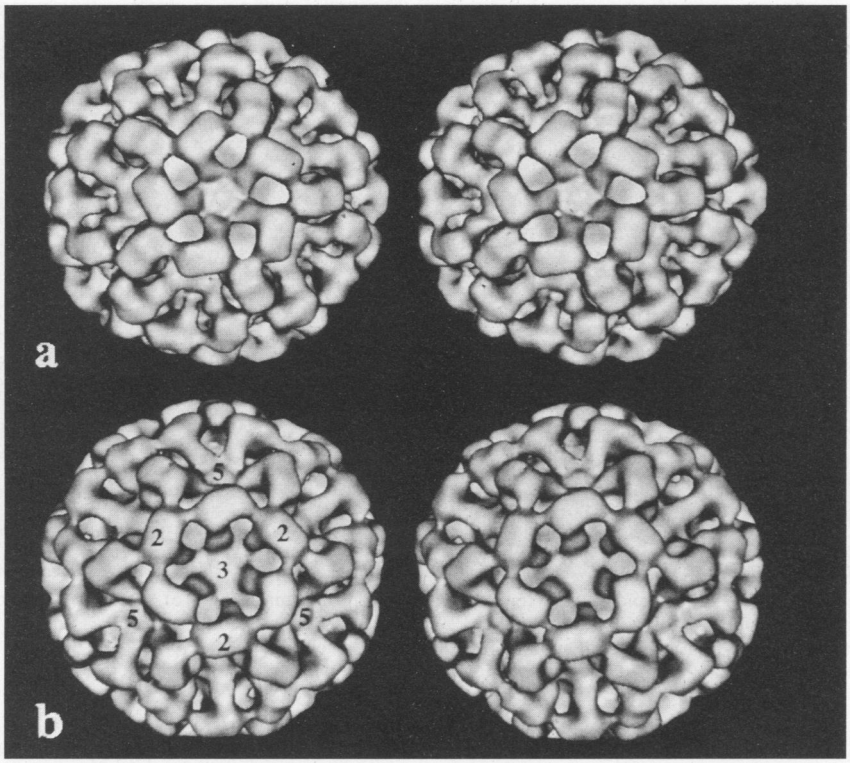

FIG. 4. Stereo pairs of the three-dimensional structure of the rNV capsid viewed along the icosahedral 5-fold (a) and 3-fold (b) axes. (b) Icosahedral symmetry (5, 3, and 2) axes are indicated.

Capsomeres are dimers of the capsid protein. Mass density calculations of the entire capsid, assuming a molecular mass of 58 kDa and a protein density of 1.30 g/cm^3, agree well with 180 molecules of the coat protein. In the T=3 structure of rNV particles, there are 90 arch-like capsomeres at all the local and strict 2-fold axes. The mass density calculations and the locations of the capsomeres on the icosahedral lattice and their shapes strongly indicate that the capsomeres represent dimers of the coat protein. Each side of the arch then represents a single molecule of the coat protein. Dimeric clustering of the coat protein is a common feature in the T=3 virus structures.

The coat protein structure. The A1, A2, and B1 sides of the arch-like capsomeres, each representing a coat protein molecule, constitute the three quasiequivalent subunits of the T=3 structure. The rest of the subunits in the structure are equivalent to one of these three subunits related by the icosahedral symmetry. These subunits have similar structures: the distal globular head domain, called P2, which appears bilobed; a

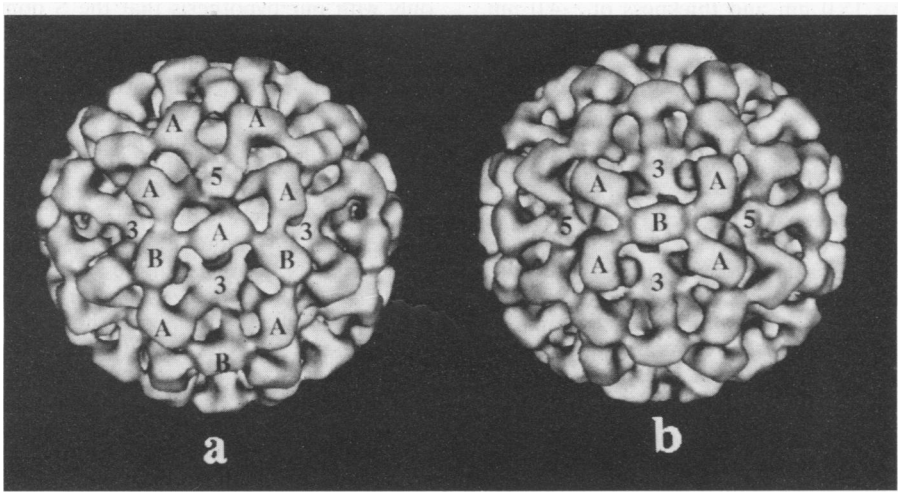

FIG. 5. Surface representations of the three-dimensional structure viewed along the local 2-fold axis (a) and the icosahedral 2-fold axis (b). Two types of capsomeres, A and B, and a set of icosahedral symmetry axes are marked. In each particle, there are 60 type A capsomeres and 30 type B capsomeres related by the icosahedral symmetry axes.

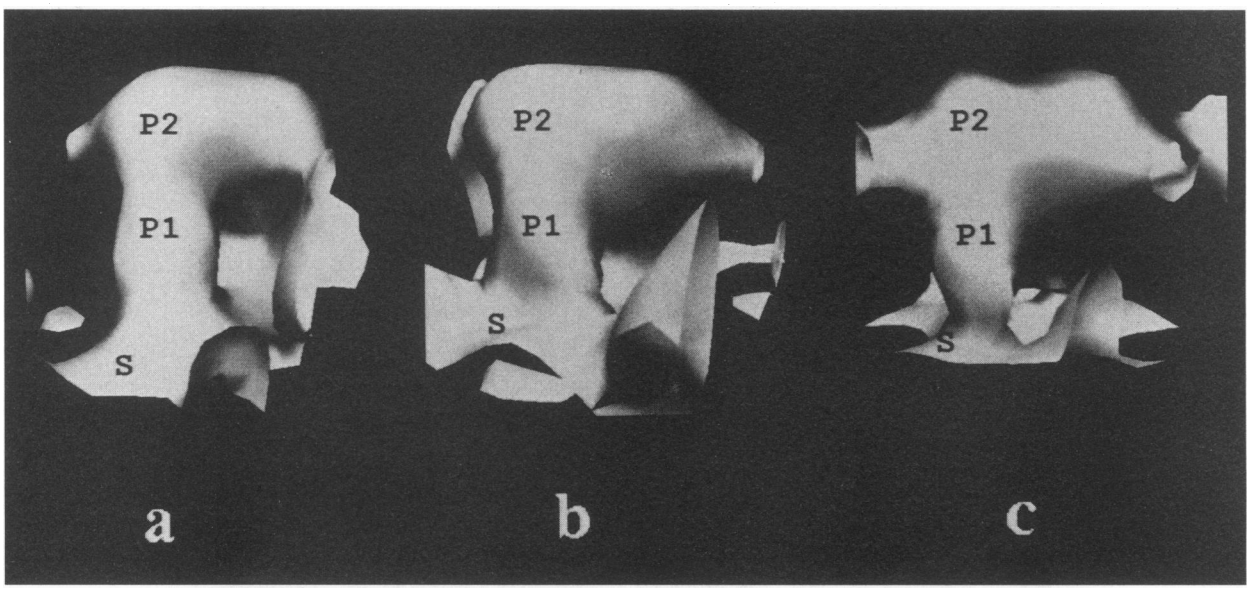

FIG. 6. Each side of the type A arch, A1 (a) and A2 (b), represent a capsid protein molecule. (c) One side of the type B arch, B1, is shown. The other side is equivalent to this side because of the icosahedral 2-fold axis. The three domains, P1, P2, and S, in these coat proteins are indicated. A1, A2, and B1 are the three quasiequivalent subunits of the capsid structure.

stem domain, called P1; and a shell domain, called S. These domains are so named by following the convention used in describing the coat protein structure in TBSV, TCV, and other T=3 structures (20, 47).

The projecting P (P1 + P2) domains in the rNV capsid protein are significantly longer than those in TBSV or TCV. The P domains in these plant viruses are about 2.5 nm in length compared with about 4.5 nm in the rNV capsid. The longer projection in rNV (and hence greater radius) can be attributed to the larger molecular weight of the coat protein. In contrast to the arch-like formation of the projecting domains in the rNV particles, in TBSV and TCV, the P domains oppose each other rather closely to appear more like a cylinder.

The S domains of the rNV subunits merge together to form the continuous mass density that is found between the radii of 11.0 and 15.0 nm. It is interesting that the dimensions of the shell, i.e., the radius of 15.0 nm and thickness of ~4.0 nm, formed by the S domains in rNV particles, are very similar to those found in TBSV, TCV, and other T=3 viruses such as SBMV, Flock House virus, and black beetle virus. The capsid proteins of the latter viruses have only the S domain (47).

β-Barrel motif. The S domains of the capsid proteins in the T=3 plant and insect viruses have a common central structural motif called the eight-strand β-barrel (20, 47). The wedge-shape β-barrel motif appears ideal to form the contiguous shell. The similarity in the dimensions of the shell between these viruses and the rNV capsid has prompted us to speculate that the S domain of the rNV capsid protein may fold into an eight-strand β-barrel structure. The β-barrel structure also is found in the VP1, VP2, and VP3 structures of picornaviruses. The structures of VP1, VP2, and VP3 in picornaviruses, analogous to the S domains of the three quasiequivalent subunits in the T=3 structures, form rather a contiguous shell, with a radius of ~15.0 nm and a thickness of 4.0 nm, without any prominent protrusions (19, 47). Comoviruses also have a contiguous shell of similar dimensions formed by 180 β-barrels (9).

Possible domain organization along the peptide sequence. An interesting question is what regions in the amino acid sequence of the Norwalk capsid protein constitute the S and P domains. When we examine the capsid protein sequences of the Norwalk and Norwalk-like viruses, the most conserved region occurs between the amino acid residues 30 and 250 (29, 34, 52). The C-terminal regions exhibit significant variation. It has been noticed that the region between residues 30 and 250 exhibit a weak homology with the VP3 sequences of picornaviruses. Particularly interesting is the conservation of the PPG tripeptide not only in these sequences but also in the animal calicivirus sequences (29, 38–41). This PPG sequence is found at the terminus of the E strand of the eight-strand (BIDG CHEF strands) β-barrel in the picornavirus structures.

It is quite possible that the N-terminal 250 residues constitute the S domain and the P1 and P2 domains are formed by the residues beyond 250. Such a proposition is consistent not only with our hypothesis that the S domain may fold into a β-barrel but also with the mass density calculations (assuming a density of 1.30 g/cm^3 and 180 molecules of the capsid protein) that indicate that molecular masses of the S domain and of the P1 and P2 together are 25 and 33 kDa, respectively. Such an organization of the domain structures, along the amino acid sequence of the Norwalk capsid protein, would be in some respects similar to that found in TBSV and TCV. In the TBSV and TCV structures, the P domain is formed by the C-terminal 114 residues, while the S domain is found more towards the N terminus. In these structures, in addition to the P and S domains, there is another domain which is internal, called the R domain, formed by the first 80 N-terminal residues (21, 24). The Norwalk capsid protein sequence does to have such a basic N terminus region (29, 34, 52).

Hinge region. When we compare the structures of the isolated subunits, A1, A2, and B1 (Fig. 6), the B1 subunit shows a noticeable difference from A1 and A2, particularly in the region between P1 and S domains. At this position in A1, the mass density is rather thin; however, in A1 and A2 such a thinning is not seen. Furthermore, there appear to be small, but noticeable, differences in the relative orientations of the P

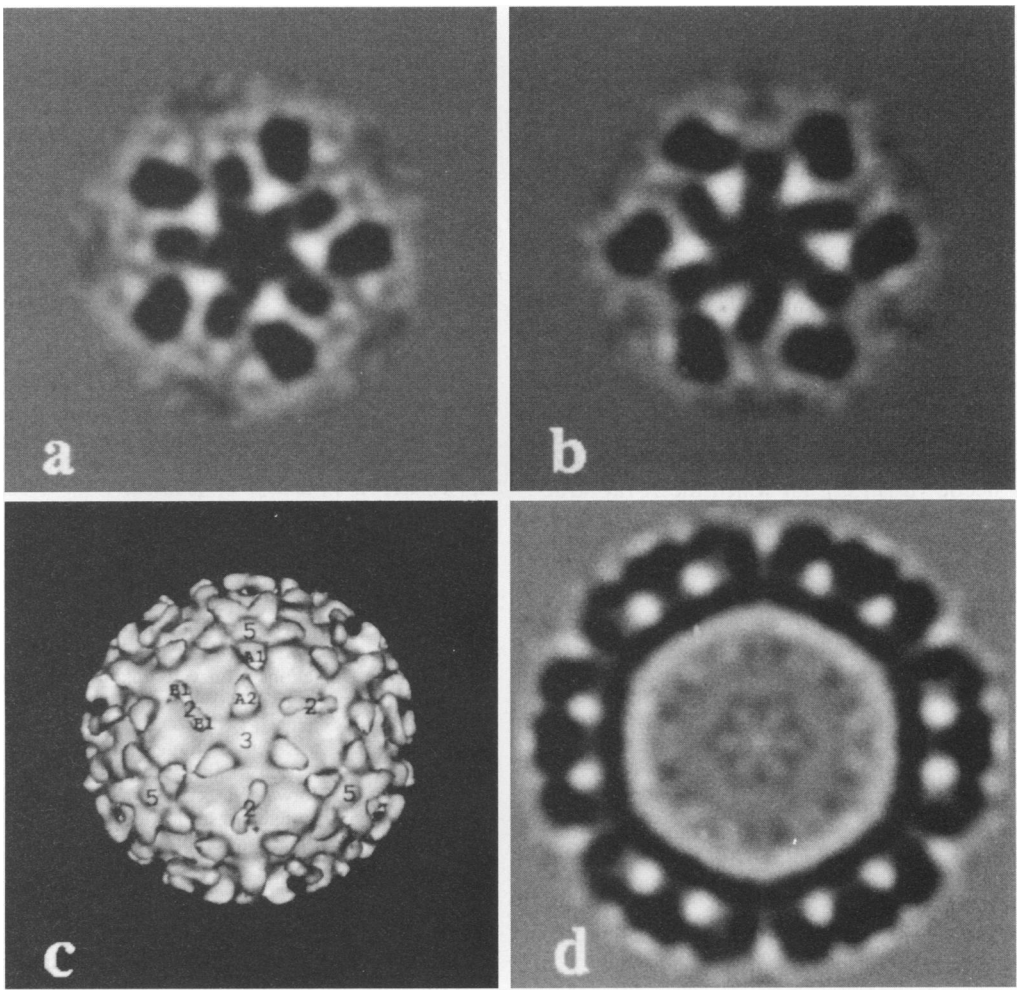

FIG. 7. Close association of the lower domains (S domains) of the capsid subunits in the inner shell. (a) Section, perpendicular to the 5-fold axis, at approximately the 15.0-nm radius, extracted from the three-dimensional map. The S domains of the A1 subunits which surround the 5-fold axis converge to form the base of the hollow at the 5-fold axis. (b) A section from the three-dimensional map at the same radius as above but perpendicular to the icosahedral 3-fold axis. The S domains from the alternating three A2 and three B1 subunits associate to form the base of the hollow at the 3-fold axis. (c) Surface representation of the three-dimensional structure at a radius of 16.0 nm along the icosahedral 3-fold axis. Only the upper hemisphere is displayed for clarity. The locations of the lower portions of A1 and A2 of a type A capsomere and two B1s of a type B capsomere are shown. Also marked are icosahedral 5-fold axes and two icosahedral 3-fold axes. (d) A central section along the icosahedral 3-fold axis. The S domains associate to form a contiguous shell of thickness 4.0 nm from which the arches emanate. (a, b, and d) Dark regions correspond to the regions of higher scattering density (i.e., proteins), and lighter regions represent the regions of lower scattering density (i.e., solvent).

domains with respect to the corresponding S domains in these subunits. It is quite possible that the capsid protein has a hinge region which enables the P (P1 + P2) domain to adapt to various quasiequivalent environments as seen in the capsid protein structures of TBSV and TCV structures. In these plant viruses, the P and S domains are connected by a hinge peptide (21, 24). Because of the tight association of the S domains to form the contiguous shell in the Norwalk virus capsid, it is difficult to visualize at this resolution how these domains adapt to the quasiequivalent environments.

Assembly strategies. In the case of TBSV, TCV, and SBMV, it has been suggested that the icosahedral structure is assembled from preformed dimers (19, 46, 49, 53). The three-dimensional structure of the rNV capsid suggests that preformed dimers are a distinct possibility. We see extensive contacts between the dimeric subunits, particularly between the P2 domains, which form the top portion of the arch, and

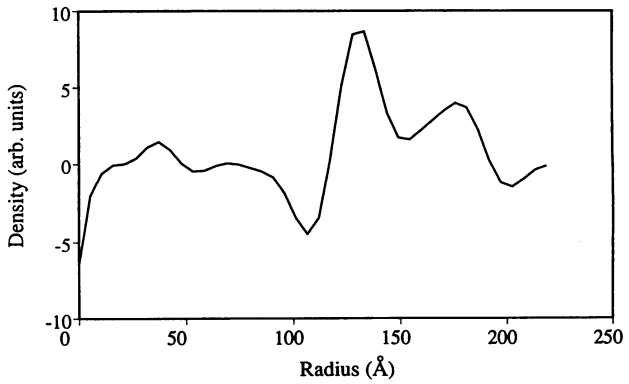

FIG. 8. Radial density profile calculated from the three-dimensional density map. The mass density corresponding to the capsid is between the radii of 11.0 and 14.0 nm. No significant mass density is seen below the radius of 11.0 nm. 1 Å = 0.1 nm.

also between the S domains in the capsid shell. However, as yet, there is no biochemical evidence for the existence of preformed dimers of the Norwalk virus capsid protein.

Another interesting question relates to the packaging of RNA into the Norwalk virus structure. The absence of any holes in the capsid structure argues against encapsidation of viral RNA after the assembly of the capsid structure has taken place. It is quite possible that the encapsidation of RNA is concomitant with the assembly of the icosahedral capsid. In the plant viruses such as TBSV, TCV, and SBMV, cocondensation of RNA with polymerizing capsid protein during the shell formation has been suggested as the most likely mechanism for RNA packing. While in TBSV and TCV, the initial protein-RNA complex has been suggested to involve trimers of dimers (19, 53), in SBMV pentamers of dimers have been proposed (46). In these interactions, the basic N-terminal R domain plays a crucial role. Other ssRNA icosahedral viruses that have N-terminal basic domains include satellite tobacco necrosis virus (36); black beetle virus (25), for which the X-ray structures have been determined; brome mosaic virus; and cowpea chlorotic mottle virus (12, 48). In several of these viruses, it has been shown that protease digestion that removes the N-terminal domain renders the virus incapable of in vitro assembly with RNA (14, 48, 49, 51). The lack of such a highly basic N-terminal region in the Norwalk virus capsid protein may indicate that the mechanism of RNA encapsidation is different from that proposed for either TBSV or SBMV.

Another interesting feature of the Norwalk virus capsid protein, as this study has shown, is its ability to form empty T=3 capsids, presumably in the absence of RNA. In this regard, Norwalk virus is similar to tymoviruses and comoviruses. These viruses also do not have the basic amino terminus and they readily form empty capsid shells (4, 9, 47). Further biochemical studies are required before the assembly mechanism for Norwalk viruses will be understood.

ACKNOWLEDGMENTS

We thank W. Chiu for helpful discussions.

This work was partly supported by NIH grants GM41064, AI36040, and AI UO130448 and by the Welch Foundation. We acknowledge the use of the electron microscope and computing facility at the 3DEM Resource Center, supported by NIH grant RR0225 and the W. M. Keck Foundation.

REFERENCES

1. **Abad-Zapatero, C., S. S. Abdel-Meguid, J. E. Johnson, A. G. W. Leslie, I. Rayment, M. G. Rossmann, D. Suck, and T. Tsukihara.** 1980. Structure of southern bean mosaic virus at 2.8 Å resolution. Nature (London) **286:**33–39.
2. **Acharya, R., E. Fry, D. Stuart, G. Fox, D. Rowlands, and F. Brown.** 1989. The three-dimensional structure of foot-and-mouth disease virus at 2.9 Å resolution. Nature (London) **337:**709–716.
3. **Adrian, M., J. Dubochet, J. Lepault, and A. W. McDowall.** 1984. Cryo-electron microscopy of viruses. Nature (London) **308:**32–36.
4. **Argos, P., and J. E. Johnson.** 1984. Chemical stability in simple spherical plant viruses, p. 1–43. *In* A. McPherson (ed.), Biological macromolecules and assemblies, vol. 1. John Wiley & Sons, Inc., New York.
5. **Baker, T. S., J. Drak, and M. Bina.** 1988. Three-dimensional structure of SV40. Proc. Natl. Acad. Sci. USA **85:**422–426.
6. **Blacklow, N. R., and H. R. Greenberg.** 1991. Viral gastroenteritis. N. Engl. J. Med. **325:**252–253.
7. **Carter, M. J., I. D. Milton, and C. R. Madley.** 1991. Caliciviruses. Rev. Med. Virol. **1:**177–186.
8. **Caspar, D. L. D., and A. Klug.** 1962. Physical principles in the construction of regular viruses. Cold Spring Harbor Symp. Quant. Biol. **27:**1–32.
9. **Chen, Z., C. Stauffacher, Y. Li, T. Schmidt, W. Bomu, G. Kamer, M. Shanks, G. Lomonossoff, and J. E. Johnson.** 1989. Protein-RNA interactions in an icosahedral virus at 3.0 Å resolution. Science **245:**154–159.
10. **Crowther, R. A.** 1971. Procedures for three-dimensional reconstruction of spherical viruses by Fourier synthesis from electron micrographs. Proc. R. Soc. Lond. Ser. B **261:**221–230.
11. **Crowther, R. A., D. J. DeRosier, and A. Klug.** 1970. The reconstruction of a three-dimensional structure from projections and its application to electron microscopy. Proc. R. Soc. Lond. Ser. B **317:**319–340.
12. **Dasgupta, R., and P. Kaesberg.** 1982. Complete nucleotide sequence of the coat protein messenger RNAs of brome mosaic virus and cowpea chlorotic mottle virus. Nucleic Acids Res. **10:**703–713.
13. **Dubochet, J., M. Adrian, J. J. Chang, J. C. Homo, J. Lepault, A. W. McDowall, and P. Schultz.** 1988. Cryo-electron microscopy of vitrified specimens. Q. Rev. Biophys. **21:**129–228.
14. **Erickson, J. W., and M. G. Rossmann.** 1982. Assembly and crystallization of T=1 icosahedral particle from trypsinized southern bean mosaic virus coat protein. Virology **116:**128–136.
15. **Fisher, A. J., and J. E. Johnson.** 1993. Ordered duplex RNA controls the capsid architecture of an icoshedral animal viruses. Nature (London) **361:**176–179.
16. **Fuller, S. D.** 1987. The T=4 envelope of Sindbis virus is organized by interactions with a complementary T=3 capsid. Cell **48:**923–934.
17. **Gray, J. J., X. Jiang, P. Morgan-Capner, U. Desselberger, and M. K. Estes.** 1993. The prevalence of antibody to Norwalk virus in England. Detection by enzyme-linked immunosorbent assay with baculovirus-expressed Norwalk capsid antigen. J. Clin. Microbiol. **31:**1022–1025.
18. **Green, K. Y., J. F. Lew, X. Jiang, A. Z. Kapikian, and M. K. Estes.** 1993. A comparison of the reactivities of baculovirus-expressed recombinant Norwalk virus capsid antigen with those of the native Norwalk virus antigen in serologic assays and some epidemiologic observations. J. Clin. Microbiol. **31:**2185–2191.
19. **Harrison, S. C.** 1984. Multiple methods of subunit association in the structure of simple spherical viruses. Trends Biochem. Sci. **9:**345–351.
20. **Harrison, S. C.** 1990. Principles of virus structure, p. 37–71. *In* B. N. Fields, D. M. Knipe, R. M. Channock, J. Melnick, B. Roizman, and R. Shope (ed.), Virology, vol. 1, Raven Press, New York.
21. **Harrison, S. C., A. Olson, C. E. Schutt, F. K. Winkler, and G. Bricogne.** 1978. Tomato bushy stunt virus at 2.9 Å resolution. Nature (London) **276:**368–373.
22. **Hendry, D. A.** 1991. Nodaviridae in invertebrates, p. 227–276. *In* E. Kurstak (ed.), Viruses of invertebrates. Marcel Dekker, Inc., New York.
23. **Hogle, J. M., M. Chow, and D. J. Filman.** 1985. Three-dimensional structure of poliovirus at 2.9 Å resolution. Science **229:**1358–1365.
24. **Hogle, J. M., A. Maeda, and S. C. Harrison.** 1986. The structure and assembly of turnip crinkle virus I: X-ray crystallographic analysis at 3.2 Å. J. Mol. Biol. **191:**625–638.
25. **Hosur, M. V., T. Schmidt, R. C. Tucker, J. E. Johnson, T. M. Gallaghar, B. H. Selling, and R. R. Rueckert.** 1987. Structure of an insect virus at 3.0 Å resolution. Proteins **2:**167–176.
26. **Hyams, K. C., J. K. Malone, A. Z. Kapikian, M. K. Estes, X. Jiang, A. L. Bourgeois, S. Paparello, and K. Y. Green.** 1993. Norwalk virus infection among desert storm troops. J. Infect. Dis. **167:**986–987.
27. **Jiang, X., D. Y. Graham, K. Wang, and M. K. Estes.** 1990. Norwalk virus genome: cloning and characterization. Science **250:**1580–1583.
28. **Jiang, X., M. Wang, D. Y. Graham, and M. K. Estes.** 1992. Expression, self-assembly, and antigenicity of the Norwalk virus capsid protein. J. Virol. **66:**6527–6532.
29. **Jiang, X., M. Wang, K. Wang, and M. K. Estes.** 1993. Sequence and genomic organization of Norwalk virus. Virology **195:**51–61.
30. **Kapikian, A. Z., and C. M. Chanock.** 1990. Caliciviridae, p. 671–693. *In* B. N. Fields, D. M. Knipe, R. M. Channock, J. Melnick, B. Roizman, and R. Shope (ed.), Virology, vol. 1. Raven Press, New York.

31. **Kaplan, J. E., G. W. Gary, and R. C. Baron, et al.** 1982. Epidemiology of Norwalk gastroenteritis and role of Norwalk virus in outbreaks of acute non-bacterial gastroentertis. Ann. Intern. Med. **96:**756–761.
32. **Khan, A. S., C. L. Moe, R. I. Glass, S. S. Monroe, M. K. Estes, L. E. Chapman, X. Jiang, C. Humphrey, E. Pon, J. K. Islander, and L. B. Schonberger.** 1994. Norwalk virus-associated gastroenteritis traced to ice consumption aboard a cruise ship in Hawaii: application of molecular method-based assays. J. Clin. Microbiol. **32:**318–322.
33. **Klug, A., and J. T. Finch.** 1968. Structure of viruses of the papilloma-polyoma virus type IV. Analysis of tilting experiments in the electron microscope. J. Mol. Biol. **31:**1–12.
34. **Lew, J. F., M. Petric, A. Z. Kapikian, X. Jiang, M. K. Estes, and K. Y. Green.** 1994. Identification of minireovirus as a Norwalk-like virus in pediatric patients with gastroenteritis. J. Virol. **68:**3391–3396.
35. **Lew, J. F., J. Valdesuso, T. Vesikari, A. Z. Kapikian, X. Jiang, M. K. Estes, and K. Y. Green.** Detection of Norwalk virus infection in Finnish infants and young children. Submitted for publication.
36. **Liljas, L., T. A. Unge, K. Jones, S. Fridborg, U. Lovgren, U. Skoglund, and B. Strandberg.** 1982. Structure of satellite tobacco necrosis virus at 3.0 Å resolution. J. Mol. Biol. **159:**93–108.
37. **Luo, M., G. Vriend, G. Kamer, I. Minor, E. Arnold, M. G. Rossmann, U. Boege, D. G. Scraba, G. M. Duke, and A. C. Palmenberg.** 1987. The structure of Mengo virus at atomic resolution. Science **235:**182–191.
38. **Meyers, G., C. Wirblich, and H. J. Thiel.** 1991. Genomic and subgenomic RNAs of rabbit hemorrhagic disease virus are both protein-linked and packaged into particles. Virology **184:**677–686.
39. **Neill, J. D.** 1992. Nucleotide sequence of the capsid protein gene of two serotypes of San Miguel sea lion virus: identification of conserved and nonconserved amino acid sequences among calicivirus capsid proteins. Virus Res. **24:**211–222.
40. **Neill, J. D., I. M. Reardon, and R. L. Heinrikson.** 1991. Nucleotide sequence and expression of the capsid protein gene of feline calicivirus. J. Virol. **65:**5440–5447.
41. **Palmenberg, A. C.** 1989. Sequence alignments of picornaviral capsid proteins, p. 211–241. *In* B. L. Semler and E. Ehrenfeld (ed.), Molecular aspects of picornavirus detection and infection. American Society for Microbiology, Washington, D.C.
42. **Prasad, B. V. V., J. W. Burns, E. Marietta, M. K. Estes, and W. Chiu.** 1990. Localization of VP4 neutralization sites in rotavirus by three-dimensional cryo-electron microscopy. Nature (London) **343:**476–479.
43. **Prasad, B. V. V., P. E. Privilege, E. Marietta, R. Chen, R. O. Thomas, J. King, and W. Chiu.** 1993. Three-dimensional transformation of capsids associated with genome packaging in a bacterial virus. J. Mol. Biol. **231:**65–74.
44. **Prasad, B. V. V., S. Yamaguchi, and P. Roy.** 1992. Three-dimensional structure of single-shelled bluetongue virus. J. Virol. **66:**2135–2142.
45. **Rossmann, M. G., E. Arnold, J. W. Erickson, E. A. Frankenberger, J. P. Griffith, H. J. Hecht, J. E. Johnson, G. Kamer, M. Luo, and A. Mosser, et al.** 1985. Structure of human common cold virus and functional relationship to other picornaviruses. Nature (London) **317:**145.
46. **Rossman, M. G., and J. W. Erickson.** 1985. Structure and assembly of icosahedral shells, p. 29–73. *In* S. Casjens (ed.), Virus structure and assembly. Jones and Bartlett Publishers, Inc., Boston.
47. **Rossmann, M. G., and J. E. Johnson.** 1989. Icosahedral RNA virus structure. Annu. Rev. Biochem. **58:**533–573.
48. **Sacher, R., and P. Ahlquist.** 1989. Effects of deletions in the N-terminal basic arm of brome mosaic virus coat protein on RNA packaging and systemic infection. J. Virol. **63:**4545–4552.
49. **Sorger, P. K., P. G. Stockley, and S. C. Harrison.** 1986. Structure and assembly of turnip crinkle virus. II. Mechanism of reassembly *in vitro*. J. Mol. Biol. **191:**639–658.
50. **Treanor, J. J., X. Jiang, H. P. Madore, and M. K. Estes.** 1993. Subclass-specific serum antibody responses to recombinant Norwalk virus capsid antigen (rNV) in adults infected with Norwalk, Snow Mountain, or Hawaii virus. J. Clin. Microbiol. **31:**1630–1634.
51. **Vriend, G., M. A. Hemminga, B. J. M. Verduin, J. L. De Wit, and T. J. Schaafsme.** 1981. Segmental mobility involved in protein-RNA interaction in cowpea chlorotic mottle virus. FEBS Lett. **134:**167–171.
52. **Wang, J., X. Jaing, H. P. Madore, J. Gray, U. Desselberger, T. Ando, Y. Seto, I. Oishi, J. F. Lew, K. Y. Green, and M. K. Estes.** Sequence diversity of small round structured viruses in the Norwalk virus group. Submitted for publication.
53. **Wei, N., and T. J. Morris.** 1991. Interactions between viral coat protein and a specific binding regions on turnip crinkle virus RNA. J. Mol. Biol. **222:**437–443.